Phenomenological Model for Gas Damping of High-Speed Switches

D. S. Greywall, J. A. Walker, P. A. Busch, S. C. Arney, D. J. Bishop, G. D. Boyd,
N. J. Frigo*, K.W. Goossen, P. P. Iannone*, R. R. Ruel, and B. Yurke

Bell Laboratories, Lucent Technologies
600 Mountain Avenue, Murray Hill, NJ 07974
* AT&T Laboratories-Research
100 Schultz Drive, Red Bank, NJ 07701

ABSTRACT

This paper discusses a simple phenomenological model of squeeze-film gas damping which has been applied to the design of micromachined optical modulators operating at speeds in excess of 12Mbits/sec. The model is described by analytic expressions and does not rely on the Reynolds or Navier-Stokes equations. It shows, in particular, that to prevent ringing following a step change in driving force, devices intended to operate at speeds greater than a few Mbits/sec must be packaged at elevated gas pressure. Comparisons are made with experimental data.

Keywords: squeeze-film damping, micromachined device, optical modulator

INTRODUCTION

High-speed mechanical switches require structures with high natural resonant frequencies, a requirement that can be met easily with micromachined silicon devices. The difficulty is that as the resonant frequency is pushed into the MHz regime, stiff structures will generally oscillate following a step change in the drive signal - making them useless for any switching application. Our recent work[1], however, has shown that this ringing can be effectively controlled using only gas damping if the micromachined structures have the proper geometry and if they are packaged at elevated pressures. A specific result of these studies is an optical modulator which operates at a speed of 12 Mbits/sec. Such optical switches[2] have many potential uses including fiber-to-the home[3,4] and other remote data sensing applications[5].

A drumhead design was chosen, Fig. 1, because its symmetry minimizes stress concentration. This is important since the devices are constructed with a large intrinsic membrane stress (typically 700-1000 MPa) in order to achieve the required high speed with a rather large device. The larger size eases the constraints on fiber alignment. The cylindrical cavity under the drumhead is created by removing sacrificial material using only the damping holes to provide access for the etchant.

The thin moveable membrane has an optically active region near its center. Because the membrane thickness and the size of the gap under the membrane are both on the order of microns and so comparable to the wavelength of light, optical interference effects between the membrane and substrate are significant. Consequently a very-small displacement of the membrane can cause a dramatic change in the amount of light reflected from the surface. In the figure, light emanating from the end of an optical fiber strikes the central optical window region of the membrane at normal incidence.

The annular region surrounding the window, shown in dark shading in Fig.1, is a metal electrode which constitutes one plate of a capacitor. The second plate is the rigid, conducting, doped-silicon substrate. When a voltage is applied to the capacitor, the electrostatic force pulls the membrane towards the back plate, changing the amount of light reflected back into the

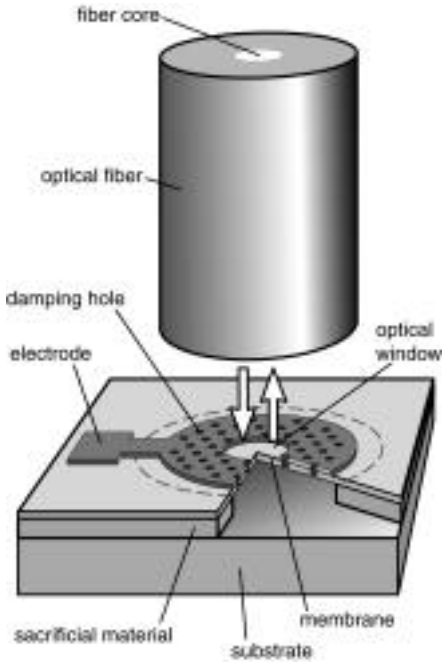

Fig. 1. Micromachined drumhead optical modulator.

fiber.

In the present geometry, the thickness of the membrane is 0.2μm, which corresponds to an optical path length of λ/4 if the optical wavelength (in vacuum) is 1.5 μm The gap spacing under the undeflected membrane is 1.0 μm, which corresponds to an optical path length of about 3λ/4. Under these conditions, the reflected beam has 70% of the amplitude of the incident beam. On the other hand, when sufficient voltage is applied to the capacitor to decrease the midpoint gap spacing to 2λ/4 there is nearly-perfect destructive interference and no light is reflected. Thus if mechanical ringing can be controlled effectively, digital information in terms of voltage can be converted directly into optical data.

MODEL

Significant insight into the damping issue was achieved using a simple model[1] which contains all of the essential elements of a gas damped device and whose behavior can be described by analytic expressions.

This model device consists of a porous piston with mass *m* and cross-sectional area *a* which is supported a distance *h* above the bottom of the cylinder by a mechanical spring with constant *k*. The restoring force is due to the mechanical spring and to the instantaneous difference between the ambient pressure P_o and the pressure within the cylinder.

The equation of motion is solved under the assumption that the rate of gas flow through the piston is proportional to the gradient in pressure. The proportionality constant ξ, which is treated as an *empirical* parameter, in general is expected to have a complicated dependence on many quantities, including the number, size, and physical arrangement of the small holes passing through the piston; the size of the gap under the piston; and the type of gas used. A further complication arises due to the fact that the mean free path of the gas molecules is comparable to the gap size. The characteristic time τ for the decay of pressure in the cylinder is related to ξ by

$$\tau = \frac{ah}{RT\xi}.$$

In addition to τ the mechanical response of the driven piston is governed by the parameters ω_o and ω_g. The quantity

$$\omega_o \equiv \sqrt{\frac{k}{m}}$$

is the natural frequency of the membrane measured in vacuum;

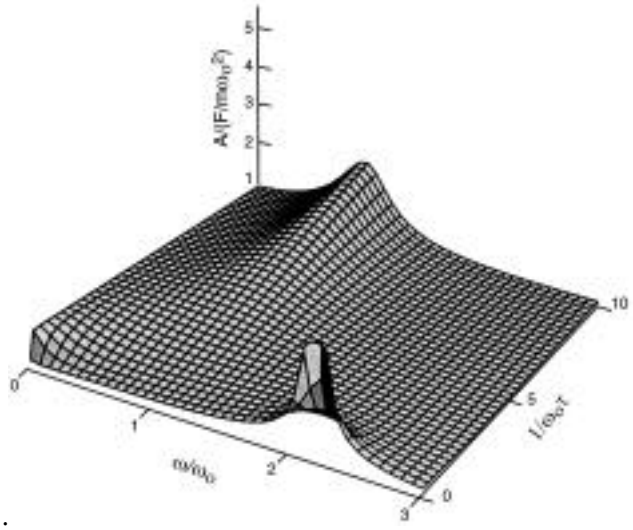

.

Fig. 2. Displacement amplitude plotted versus drive frequency and "piston porosity", all in dimensionless units. The reduced gas frequency is fixed at 2.0.

$$\omega_g \equiv \sqrt{\frac{aP_o / h}{m}}$$

is the resonant frequency that the piston would have if the restoring force were due only to the compression of the gas in the cylinder.

The expressions for the piston amplitude and phase relative to the sinusoidal drive force are

$$A = \frac{F_o / m\omega_o^2}{\sqrt{\left[1 + \frac{\omega_g^2/\omega_o^2}{1+(\omega\tau)^{-2}} - \frac{\omega^2}{\omega_o^2}\right]^2 + \left[\frac{\omega_g^2/\omega_o^2}{\omega\tau\left[1+(\omega\tau)^{-2}\right]}\right]^2}}$$

and

$$\tan\phi = \frac{\omega_g^2 / \omega\tau}{\left(\omega_o^2 - \omega^2\right)\left(1+(\omega\tau)^{-2}\right) + \omega_g^2}.$$

Response curves based on the model are shown in Fig. 2. These were computed with ω_g/ω_o fixed at 2 and using various values of the "porosity" $1/\omega_o\tau$. Note that in the extremes of either very-small or very-large "porosities" there are sharp resonance peaks. This implies ringing when the piston has either too few holes or too many holes. The higher resonant frequency in the limit of a small number of damping holes reflects the contribution of the compressed gas to the total restoring force. The featureless region at intermediate values of $1/\omega_o\tau$ suggests that there is an optimum porosity to minimize ringing, at least if ω_g/ω_o is equal to 2.

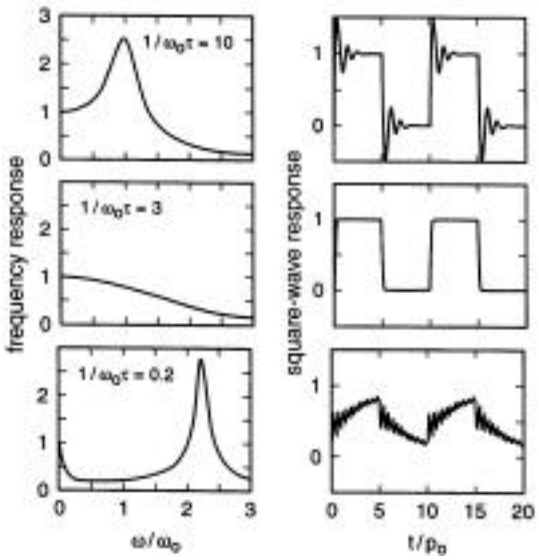

Fig. 3. Square-wave response corresponding to various frequency response curves. The calculations are for $\omega_g/\omega_o=2$ and the values of $1/\omega_o\tau$ indicated. Time for the square-wave response curves is measured in units of the natural period, $p_o=1/f_o$.

An important finding is that if ω_g/ω_o is much smaller than 2, the response curve, independent of the piston's porosity, will exhibit a resonance peak. If ω_g/ω_o is greater than 2, *and* the piston has the appropriate porosity, the frequency response will look more like that of an ordinary low-pass filter. Because ω_g/ω_o is proportional to the square root of the pressure, the constraint on this parameter means that the ambient pressure must be sufficiently high. The minimum pressure is roughly proportional to the square of the resonant frequency and exceeds atmospheric pressure for frequencies near 1MHz.

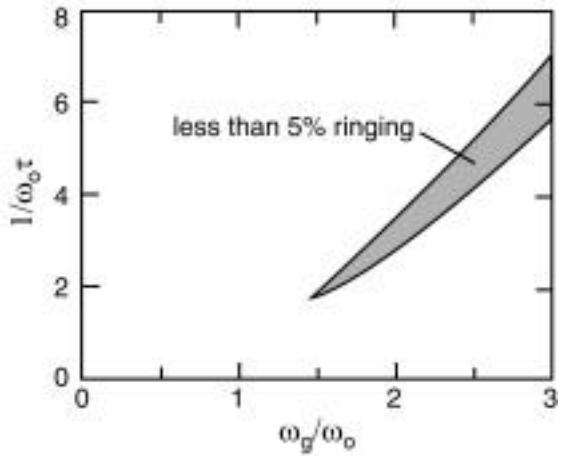

Fig. 4. Values of ω_g/ω_o and $1/\omega_o\tau$ which imply a square-wave response with less that "5% ringing."

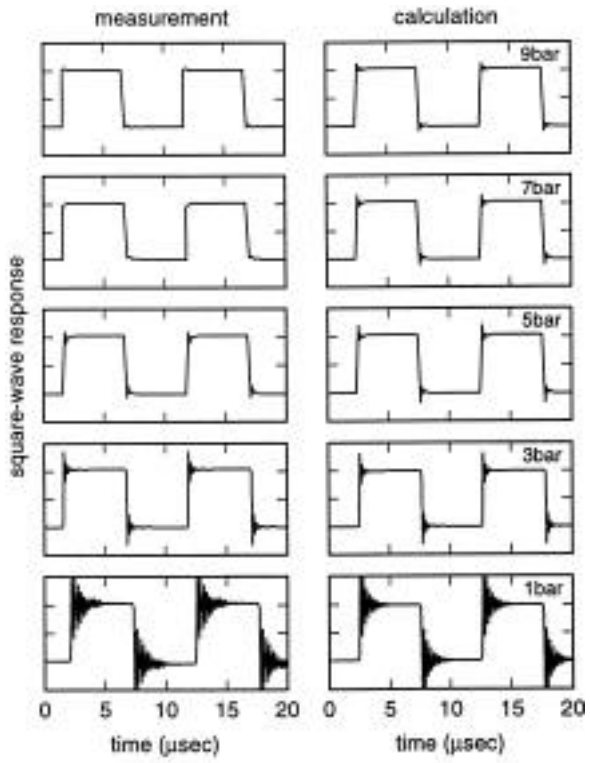

Fig. 5. Demonstration that an elevated ambient gas pressure can control switch ringing. Shown are calculated and measured square-wave response curves for the modulator in neon at various pressures.

The correspondence between frequency response and square-wave response is shown in Fig. 3 for $\omega_g/\omega_o=2$. This response was computed by simply summing the complex frequency responses corresponding to the Fourier components of a square-wave drive signal. As in Fig. 2, $\omega_g/\omega_o=2$. Having too few damping holes ($1/\omega_o\tau$ small) or too many holes leads to unacceptable behavior. The best response occurs when $1/\omega_o\tau=3$, again if $\omega_g/\omega_o=2$.

Other pairs of parameter values for ω_g/ω_o and $1/\omega_o\tau$ that give good square-wave response are indicated by the shaded region in Fig. 4. Parameters for a given device will fall in this region only if the ambient gas pressure is "high enough" and the membrane has the appropriate porosity. Experimental values for $\omega_g(P)/\omega_o$ and $1/\omega_o\tau(P)$ are determined by fitting measured frequency response curves using the functional expressions derived for the model device.

COMPARISON WITH EXPERIMENTAL DATA

The following discusses the application of the model to one specific example, the drumhead optical modulator shown schematically in Fig. 1. The device

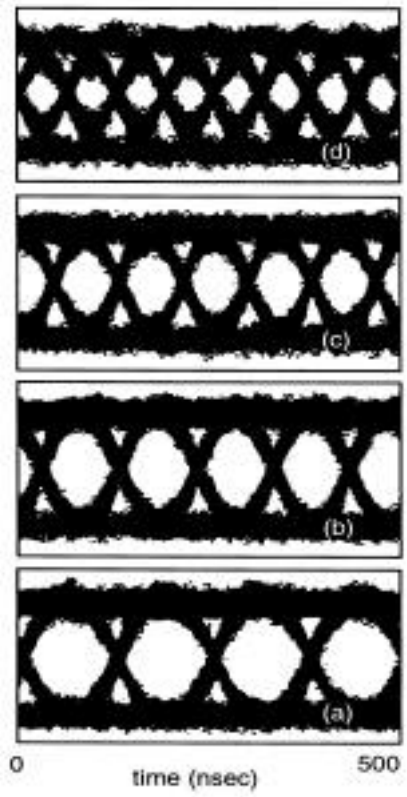

Fig. 6. Eye diagrams. In (a), (b), (c), and (d) the speeds are 8, 10, 12, and 16 Mbits/sec, respectively.

has a diameter of 110μm and a 30μm-diameter central window surrounded by 48 three-micron diameter damping holes in a close-pack pattern.

The square-wave response measured in neon gas under various pressures is shown in Fig. 5, where comparison is made with predictions based on the modeling calculations. Note that ringing is completely suppressed only when the pressure is raised above several bars (1bar=1atm).

The time measured for the response to rise from 10% to 90% of its equilibrium value in the "on" state is 85nsec, implying that this device should be capable of switching light at a speed of at least 12 Mbits/sec.

A more-direct manner of determining the quality of a data signal is by means of eye diagrams. The diagrams shown in Fig. 6 were generated by monitoring the response of the modulator to data words of pseudorandom length using on oscilloscope triggered by the clock generating the data bit rate. The patterns formed are simply the superposition of all 0-to-1 and 1-to-0 transitions, each preceded and followed by various combinations of 1 and 0 levels. Qualitatively, the more open the eye, the lower the probability for errors in the data.

SUMMARY

Micromachined switches bring together very small physical size, compatibility with on-chip silicon circuitry, and economical price, and so show great promise for many applications. The range of possibilities is expanded by the demonstration that these devices can be used for switching applications requiring speeds in excess of 12Mbits/sec.

[1] D. S. Greywall, P. A. Busch, and J. A. Walker, *Phenomenological Model for Gas Damping of Micromechanical Structures,* Sensors and Actuators A, **72**,49-70 (1999).

[2] K. W. Goossen, J. A. Walker, and S. C. Arney, *Silicon Modulator Based on Mechanically-Active Anti-Reflection Layer with 1Mbit/sec Capability for Fiber-in -the-Loop Applications*, IEEE Phot. Tech. Lett., **1**, 61-64 (1989).

[3] N. J. Frigo, *A Survey of Fiber Optics in Local Access Architectures*, Optical Fiber Telecommunications, Vol IIIA, Academic Press, 1997.

[4] L. W. Lockwood, *A Unique Fiber Optic Upstream Data System*, Communications Engineering and Design, 118-120, June 1996

[5] D. Wilson, *Optical Modulator Links Processors to Sensors*, Lightwave, 7-8 October 1996.